



Figures and figure supplements

IL18 signaling promotes homing of mature Tregs into the thymus

Cristina Peligero-Cruz et al

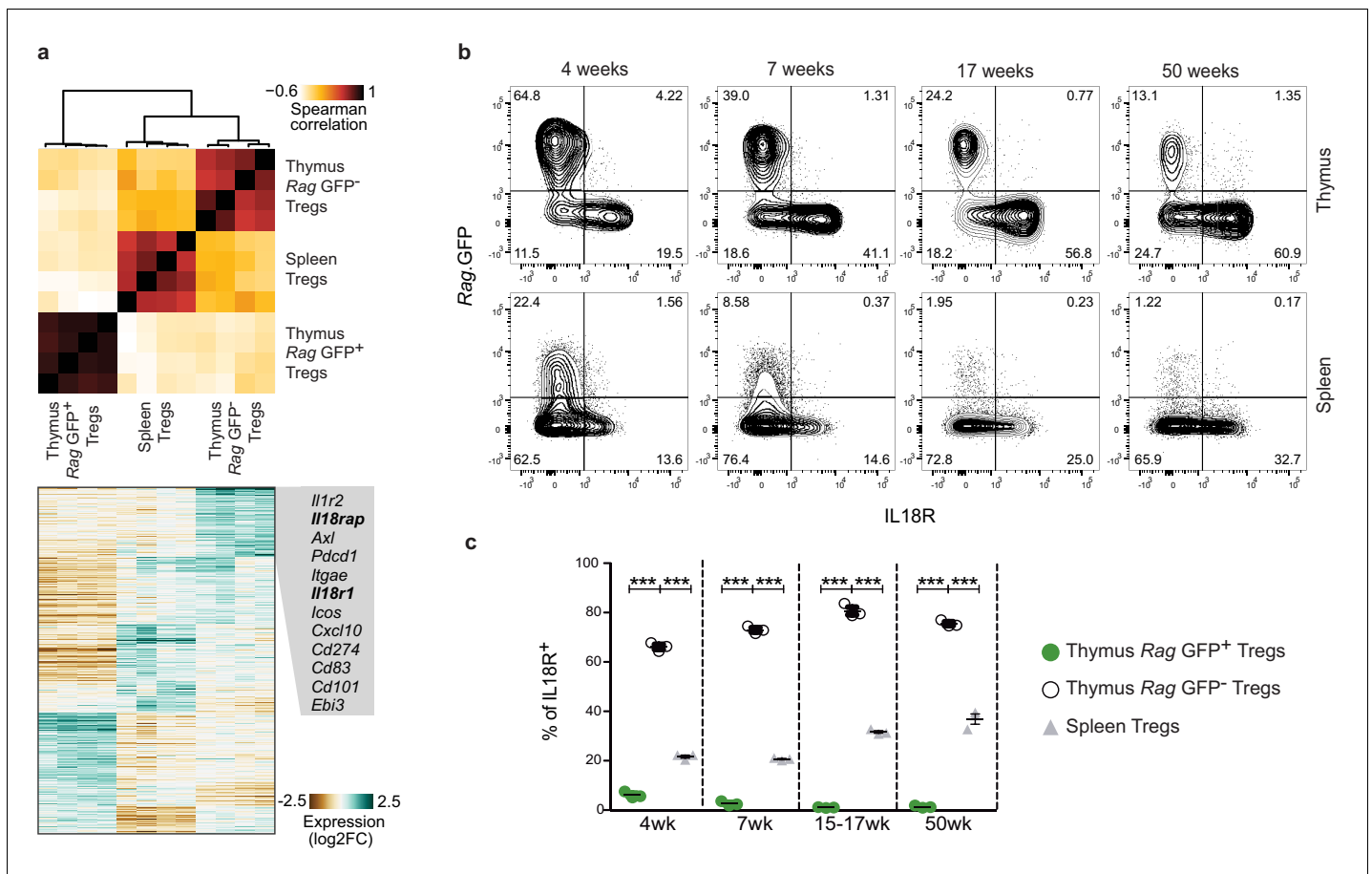


Figure 1. A subpopulation of mature Tregs in the thymus expresses IL18R. (a) Top, a heatmap showing Spearman’s correlation coefficient between different samples based on the expression of differentially expressed genes. Samples include four biological replicates each of *Rag*.GFP⁻ Tregs from the thymus, Tregs from the spleen, and *Rag*.GFP⁺ Tregs from the thymus. Bottom, a heatmap showing the normalized expression of variable genes across samples. Specific genes upregulated in *Rag*.GFP⁻ Tregs are highlighted. (b) Representative flow cytometry plot showing the expression of IL18R in Tregs from the thymus (up) and the spleen (down). Numbers indicate the percentage of cells within each gate. (c) Frequency of IL18R⁺ cells among ‘newly produced’ *Rag*.GFP⁺ Tregs in the thymus (green dots), ‘mature’ *Rag*.GFP⁻ Tregs in the thymus (white dots) and Tregs in the spleen (gray triangles) in mice from different ages. Each dot represents an individual mouse. The mean ± SEM (standard error of the mean) is shown. Data are from one representative experiment with three biological replicates. Significant differences were determined using a 2-way ANOVA, corrected for multiple comparisons by the Bonferroni method and indicated by asterisks ***p<0.001.

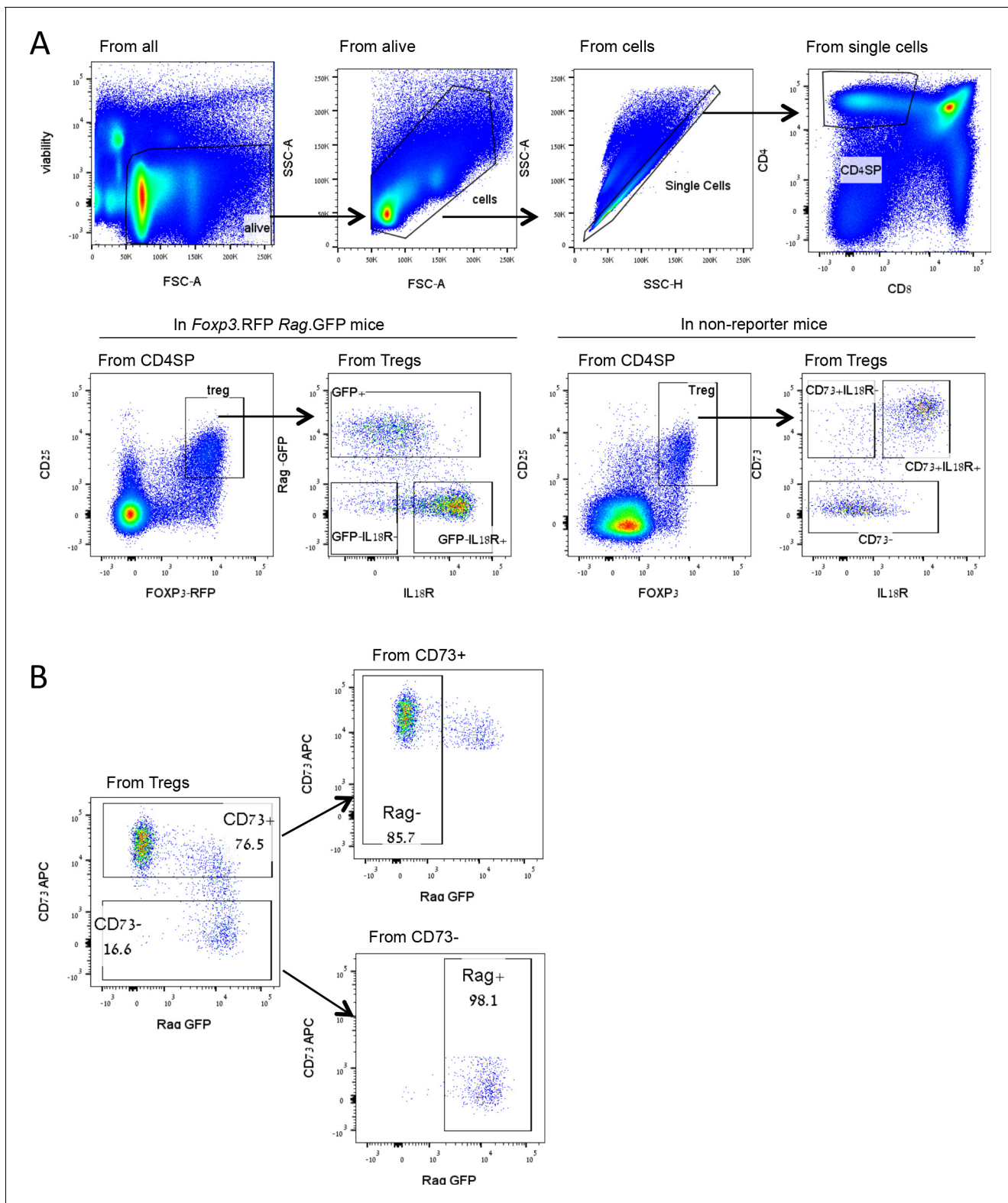


Figure 1—figure supplement 1. Treg gating strategy. (A) Representative FACS plots demonstrating the Treg gating strategy used to identify newly produced Tregs (GFP⁺ or CD73⁻) and mature Tregs (older) (GFP⁻ or CD73⁺) in the thymus of *Foxp3.RFP Rag.GFP* reporter mice or mice without reporter, respectively. (B) Validation of CD73 staining as a marker for mature Tregs in the thymus. Thymocytes of *Rag.GFP Foxp3.RFP* mice were stained with fluorescently labeled antibodies. The frequency of *Rag.GFP*⁺ or *Rag.GFP*⁻ Tregs from CD73⁺ and CD73⁻ Treg populations were analyzed. Numbers indicate the percentage of cells within each gate. Over 85% of CD73⁺ Tregs are *Rag.GFP*⁺, while over 98% of CD73⁻ Tregs are *Rag.GFP*⁺ as previously described by [Owen et al., 2019](#). Representative FACS plots from mice 8–10 weeks old are shown.

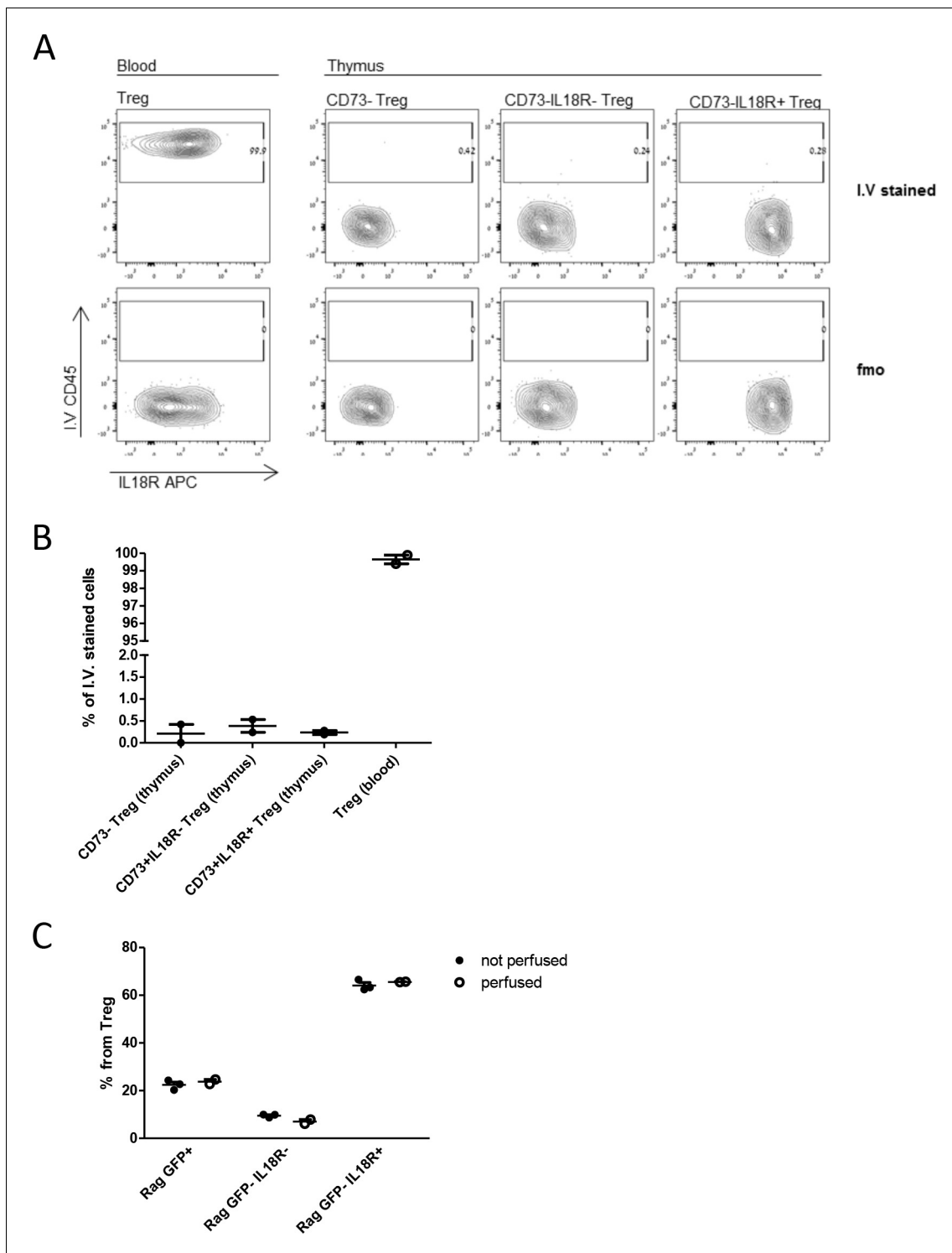


Figure 1—figure supplement 2. Mature (*Rag.GFP*⁻ or CD73⁺) Tregs are intrathymic (not a contamination from the bloodstream). (A) Representative FACS plots of intravascular CD45 staining followed by regular staining in blood and thymus. The frequency of CD45 intravascular stain (I.V.) is shown from left to right in Tregs from the blood (positive control) and from the thymus (CD73⁻ Tregs, CD73⁺IL18R⁻ Tregs, and CD73⁺IL18R⁺ Tregs). Upper panels correspond to CD45 intravascular stained mouse, while lower panels correspond to the FMO (fluorescence minus one control: mouse without CD45 intravascular staining). (B) Frequency of intravascular stained cells. (C) Frequency of *Rag.GFP*⁺ Treg, *Rag.GFP*⁻IL18R⁻ Treg, and *Rag.GFP*⁻IL18R⁺ Treg populations in the thymus of perfused and non-perfused mice. In B and C, each dot represents an individual mouse. The mean ± SEM (standard error of the mean) is shown. Data are from experiments with two biological replicates (B) and three biological replicates (C).

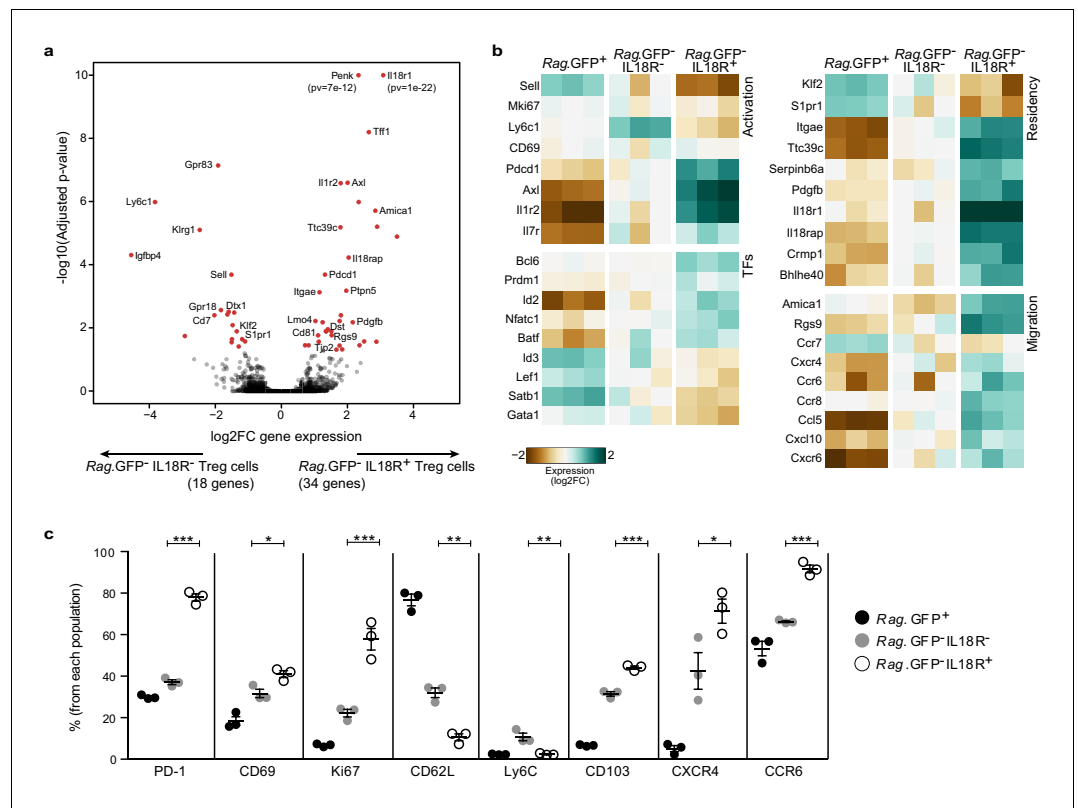


Figure 2. IL18R⁻ and IL18R⁺ represent molecularly distinct subsets of mature Tregs in the thymus. (a) A volcano plot showing differential gene expression between thymic *Rag.GFP⁺IL18R⁻* Tregs and *Rag.GFP⁺IL18R⁺* Tregs. Genes in red have an adjusted p-value < 0.05. Y axis is cut at 1e-10 for visualization. (b) A heatmap showing the normalized expression of selected variable genes in *Rag.GFP⁺* Tregs, *Rag.GFP⁺IL18R⁻* Tregs, and *Rag.GFP⁺IL18R⁺* Tregs from the thymus. (c) Frequencies of different markers analyzed using flow cytometry in *Rag.GFP⁺* Tregs, *Rag.GFP⁺IL18R⁻* Tregs, and *Rag.GFP⁺IL18R⁺* Tregs from the thymus. Each dot represents an individual mouse. The mean ± SEM (standard error of the mean) is shown. Data are from one experiment with three biological replicates. Significant differences were determined using ANOVA, corrected for multiple comparisons by the Bonferroni method and indicated by asterisks *p<0.05, **p<0.01, ***p<0.001.

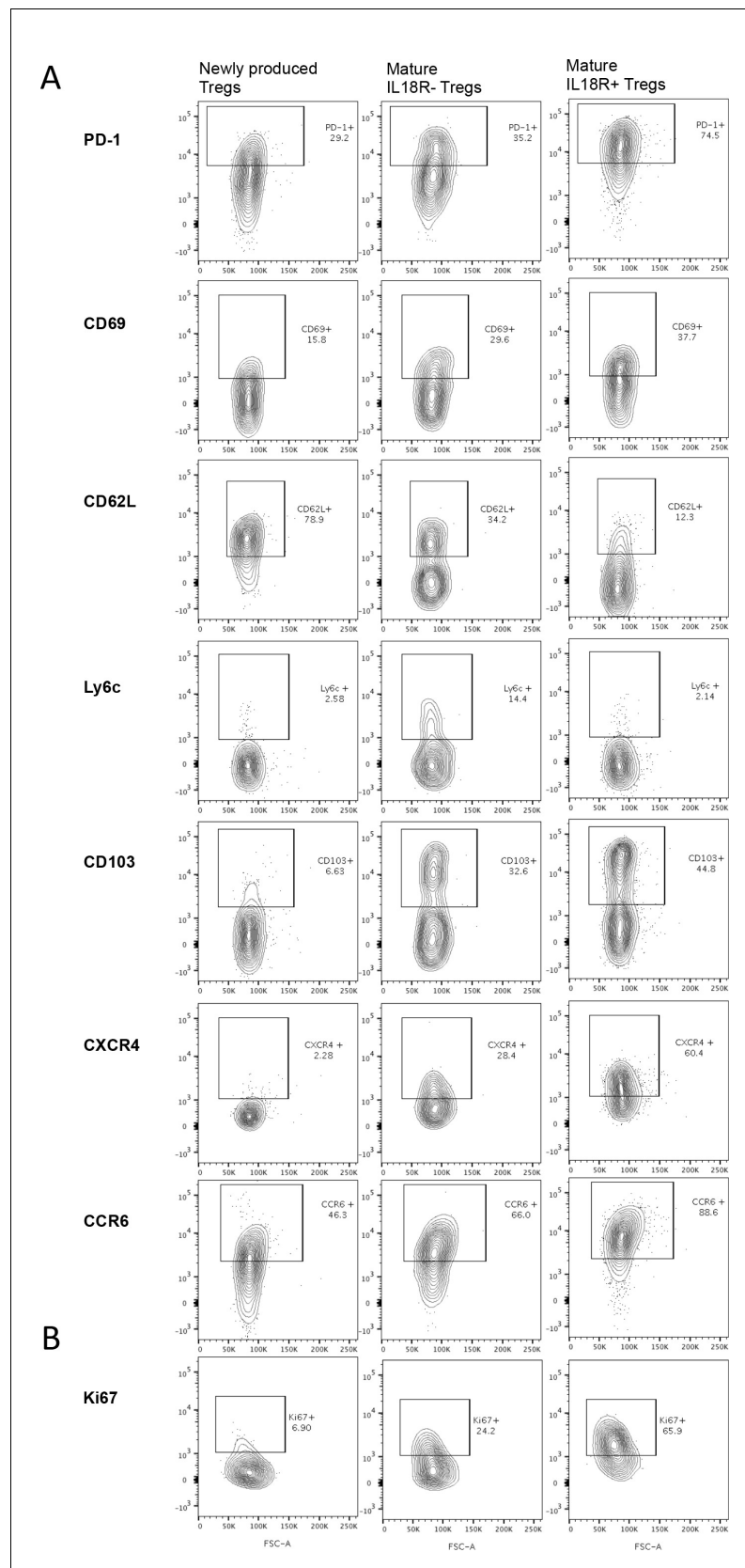


Figure 2—figure supplement 1. RNA Sequencing protein validation, Representative gating from **Figure 2c.** (A) Thymocytes of *Rag.GFP Foxp3.RFP* mice were stained with fluorescently labeled antibodies. The frequency of **Figure 2—figure supplement 1** continued on next page

Figure 2—figure supplement 1 continued

different markers in newly produced Tregs (*Rag.GFP*⁺), mature IL18R⁻ Tregs (*Rag.GFP*⁺IL18R⁻) or mature IL18R⁺ Tregs (*Rag.GFP*⁻IL18R⁺) is shown. (B) Thymocytes of wild-type mice were stained with fluorescently labeled antibodies. The frequency of intracellular Ki67 marker in newly produced Tregs (CD73⁻), mature IL18R⁻ Tregs (CD73⁺IL18R⁻), or mature IL18R⁺ Tregs (CD73⁺IL18R⁺) is shown. Numbers indicate the percentage of cells within each gate.

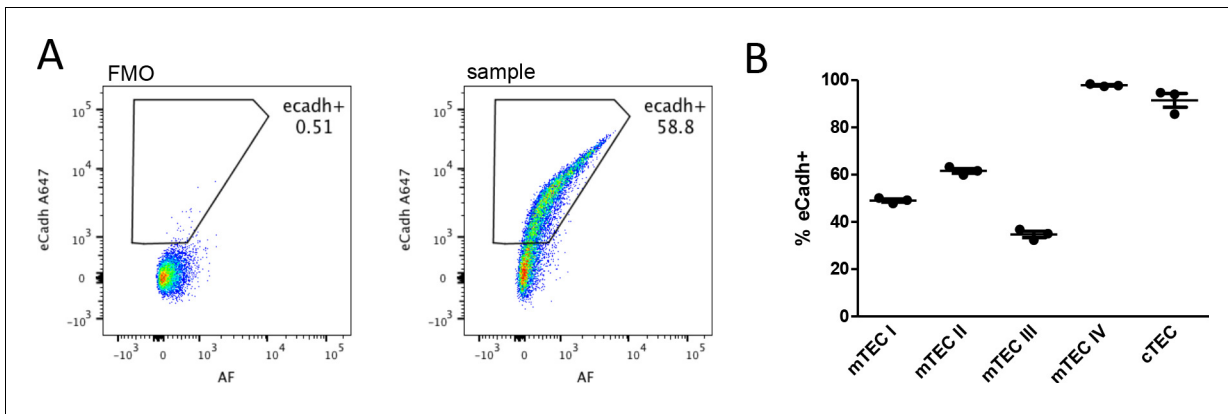


Figure 2—figure supplement 2. E-cadherin (the ligand for CD103) is expressed by thymic epithelial cells. (A) Representative FACS plots showing the expression of E-cadherin (y-axis) plotted against AF (Autofluorescence, natural fluorescence; x-axis) in total thymic epithelial cells (TEC). Numbers indicate the percentage of E-cadherin positive cells. FMO (fluorescence minus one) control (left) and sample (right) are shown. (B) Frequency of E-cadherin positive cells in different populations of thymic epithelial cells (CD45-EpCAM+): mTECI (Ly51- MHCIIIo Itgb4+), mTECII (Ly51-MHCIIhi), mTECIII (Ly51-MHCIIIo Itgb4-), mTECIV (Ly51-MHCIIIo L1CAM+), and cTEC (Ly51+). Each dot represents an individual mouse. The mean \pm SEM (standard error of the mean) is shown. Data are from one experiment with three biological replicates.

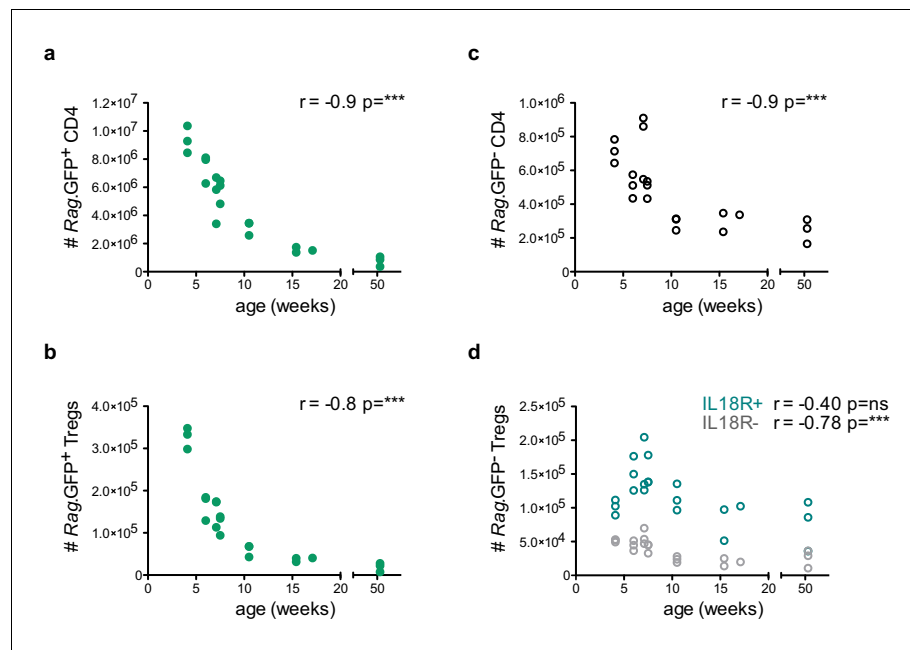


Figure 3. IL18R⁺ Tregs are resistant to age-dependent thymus involution. Thymocyte counts as a function of age in weeks. (a) Rag.GFP⁺ CD4 conventional T cells, (b) Rag.GFP⁺ Tregs, (c) Rag.GFP⁻ CD4 conventional T cells, and (d) Rag.GFP⁻ IL18R⁻ Tregs (in gray) and Rag.GFP⁻ IL18R⁺ Tregs (in blue). Each symbol represents an individual mouse. Data are from two independent experiments with 21 total mice. The Spearman’s rank correlation coefficient (*r*) and *p*-value (*p*) for the correlations between cell counts and mice age are indicated by asterisks ****p*<0.001, ns: non-significant.

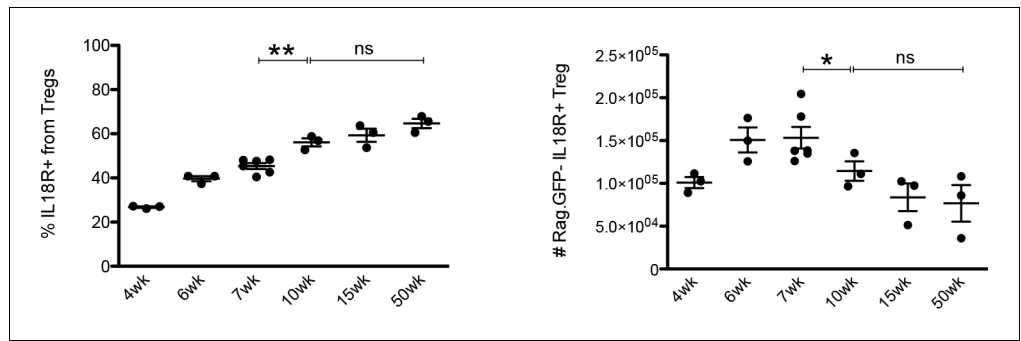


Figure 3—figure supplement 1. Frequency and counts of IL18R⁺ Rag.GFP⁻Tregs at different ages. Frequency (left) and counts (right) of IL18R⁺ Rag.GFP⁻ Tregs at different ages in Rag.GFP Fxp3.RFP mice strain. Each dot represents an individual mouse. The mean ± SEM (standard error of the mean) is shown. Data are from two experiments with three to six biological replicates. Significant differences were determined using ANOVA, corrected for multiple comparisons by the Bonferroni method and indicated by asterisks (*p<0.05,ns: non-significant).

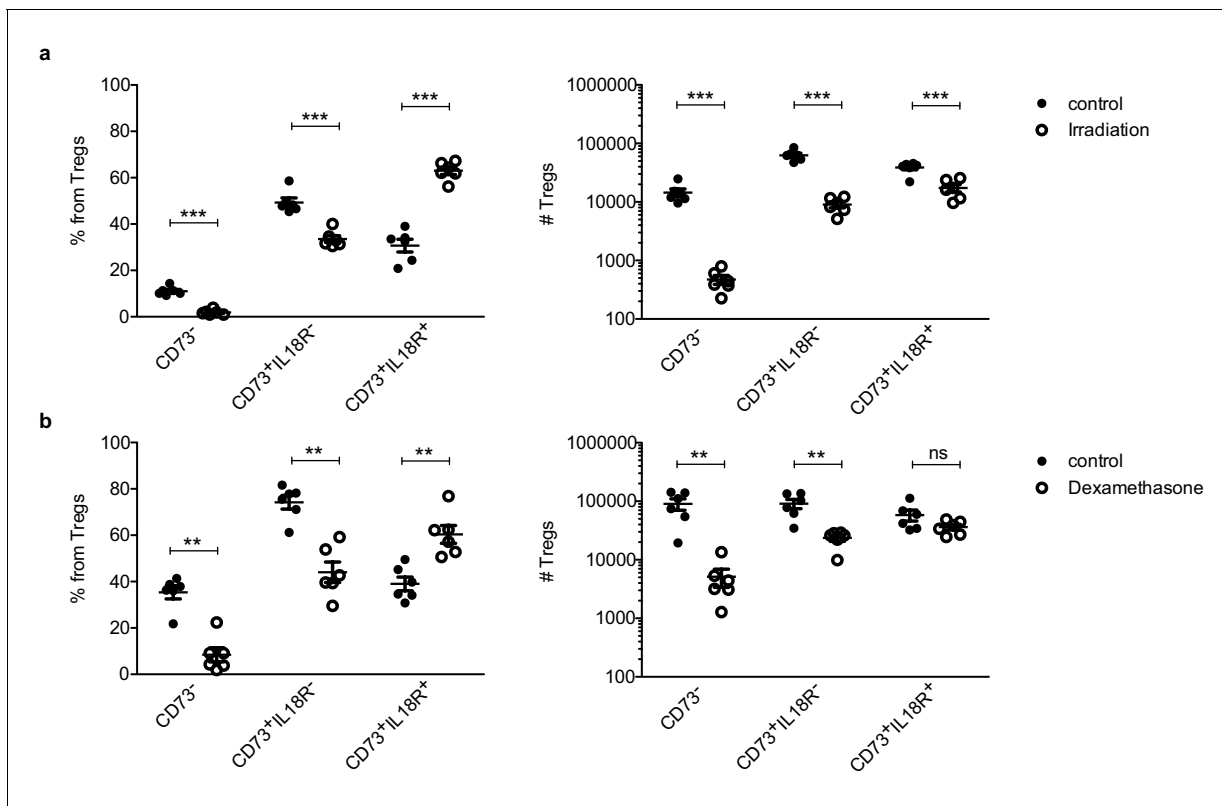


Figure 4. IL18R⁺ Tregs are resistant to stress-dependent thymus involution. Frequencies (left) and counts (right) of ‘newly produced’ CD73⁻ Tregs, ‘mature’ CD73⁺IL18R⁻ Tregs and ‘mature’ CD73⁺IL18R⁺ Tregs in control mice (solid dots) and treated mice (empty dots) upon different perturbations: (a) 7 days after 425cGy irradiation and (a) 7–10 days after 20 mg/kg dexamethasone injection. Each dot represents an individual mouse. The mean ± SEM (standard error of the mean) is shown. Data in (a,b) are from a representative experiment with six biological replicates. Significant differences were determined using 2-way ANOVA, corrected for multiple comparisons by the Bonferroni method and indicated by asterisks **p<0.01, ***p<0.001, ns: non-significant.

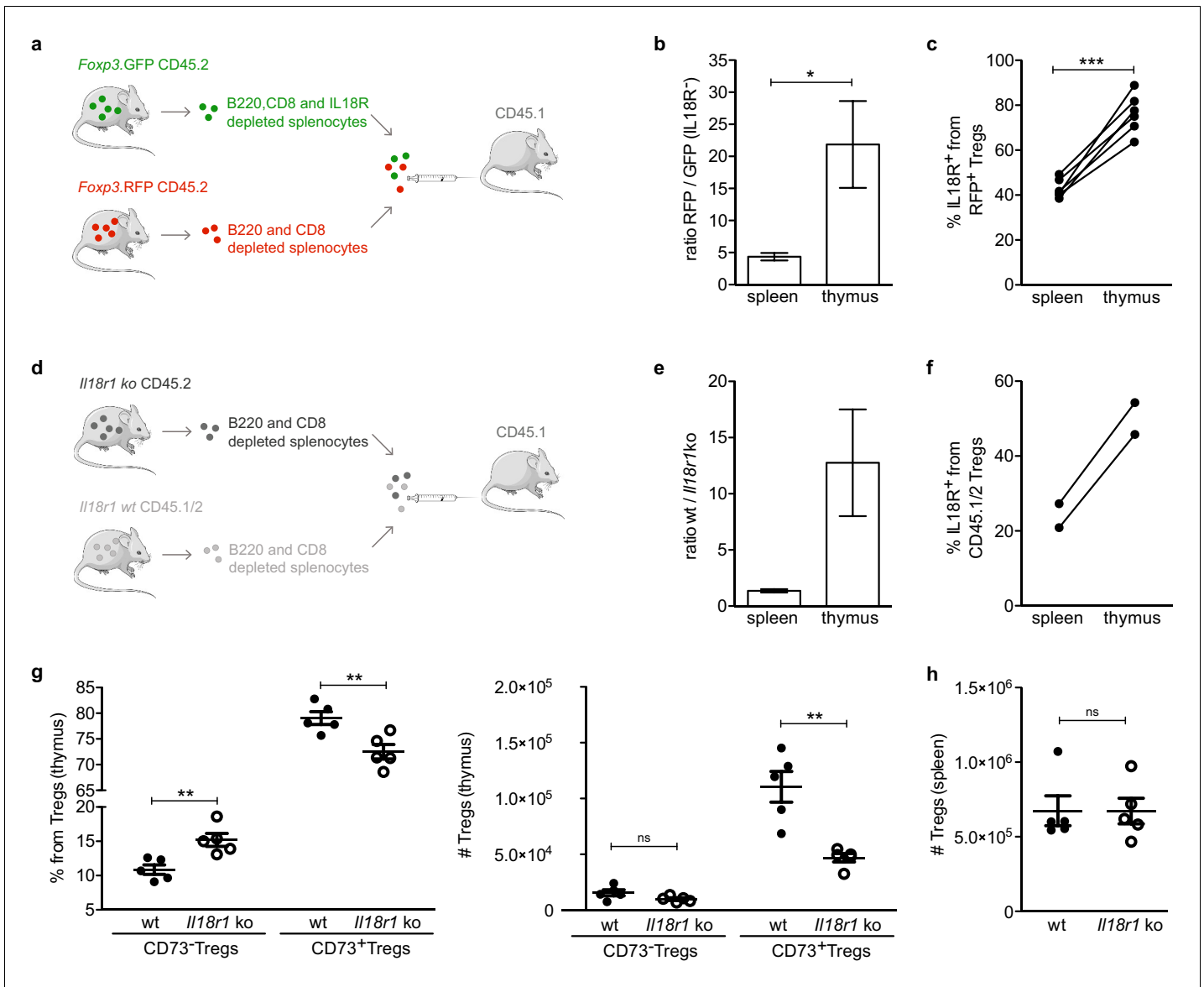


Figure 5. IL18R contributes to maintain mature Tregs in the thymus. (a) Schematic representation of the experiment in which IL18R depleted splenocytes from *Foxp3.GFP* mice were injected together with non-IL18R depleted splenocytes from *Foxp3.RFP* into CD45.1 recipients. (b) The ratio of RFP to GFP injected cells found in the spleen and thymus of recipient mice. (c) Frequency of IL18R⁺ Tregs from the *Foxp3.RFP* CD45.2 injected cells found in the spleen and thymus of recipient mice. (d) Schematic representation of the experiment in which *Il18r1*KO splenocytes were injected together with wild-type (wt) splenocytes into CD45.1 recipients. (e) The ratio of wt/*Il18r1*KO cells found in the spleen and thymus of recipient mice. (f) Frequency of IL18R⁺ Tregs from the wt injected cells found in the spleen and thymus of recipient mice. (g) Frequencies (left) and counts (right) of different Treg populations in the thymus of wt mice (solid dots) and *Il18r1*KO mice (empty dots). (h) Counts of Tregs in the spleen of wt and *Il18r1*KO mice. Each dot represents an individual mouse. The mean ± SEM (standard error of the mean) is shown. Data in (b,c) are from three independent experiments with a total of 6 biological replicates. (e,f) are from one experiment with a total of 2 biological replicates. Data in (g,h) are from one representative experiment with 12 total mice. Significant differences were determined in (b,c,e,f) using a paired t-test and in (g,h) using an unpaired t-test and indicated by asterisks *p<0.05, **p<0.01, ***p<0.001, ns: non-significant.

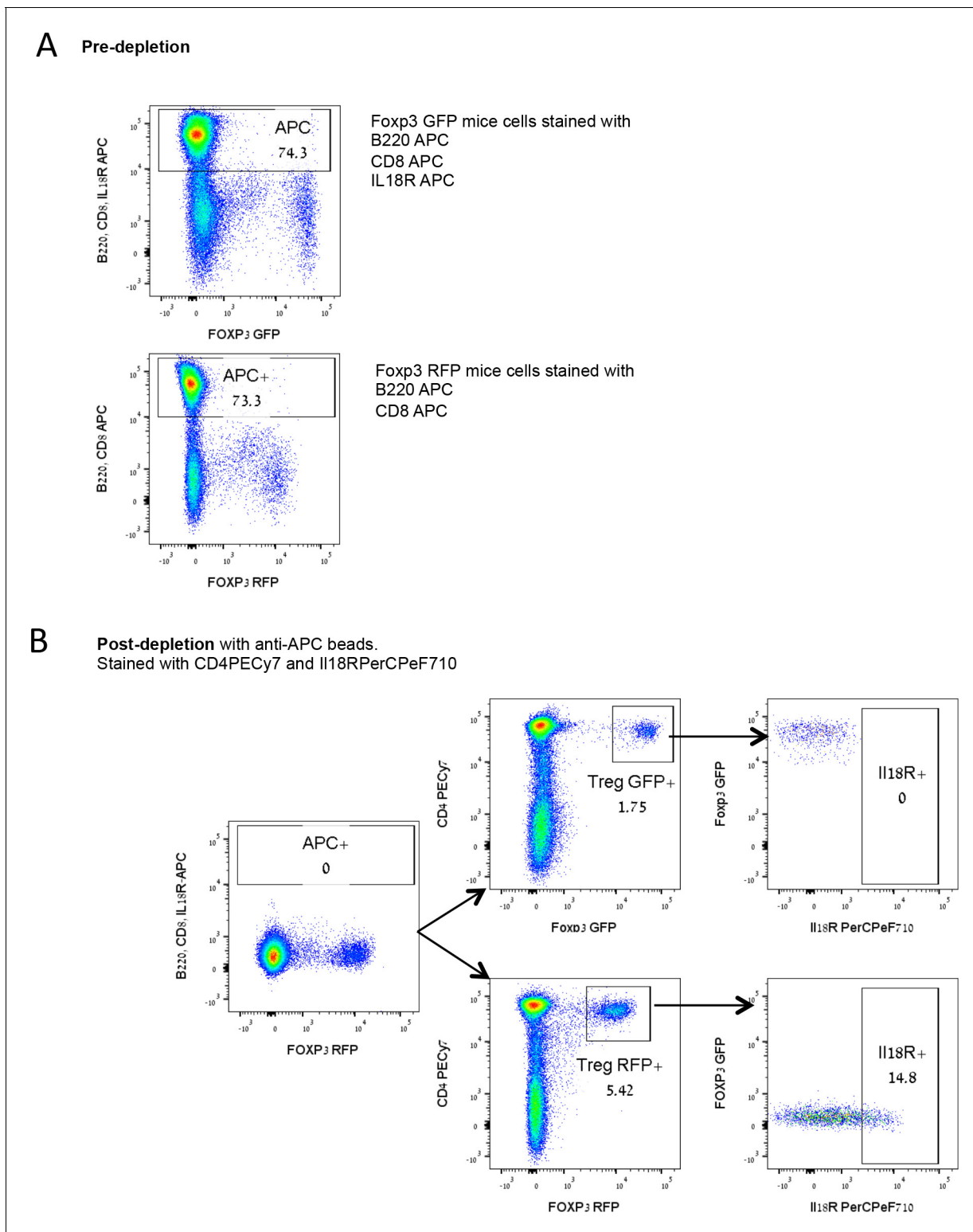


Figure 5—figure supplement 1. Purity of the injected splenocytes in the adoptive transfer experiments shown in **Figure 5**. (A) Representative FACS plots of pre-depletion samples, including pooled *Foxp3.GFP* mice splenocytes stained with B220 APC, CD8 APC, and IL18R APC (up) and *Foxp3.RFP* mice splenocytes stained with B220 APC and CD8 APC (down) (B) Representative FACS plots of post-depletion samples composed of a mix of B220-, CD8-, IL18R- depleted *Foxp3.GFP* splenocytes and B220-, CD8- depleted *Foxp3.RFP* splenocytes. Numbers indicate the percentage of cells within each gate.

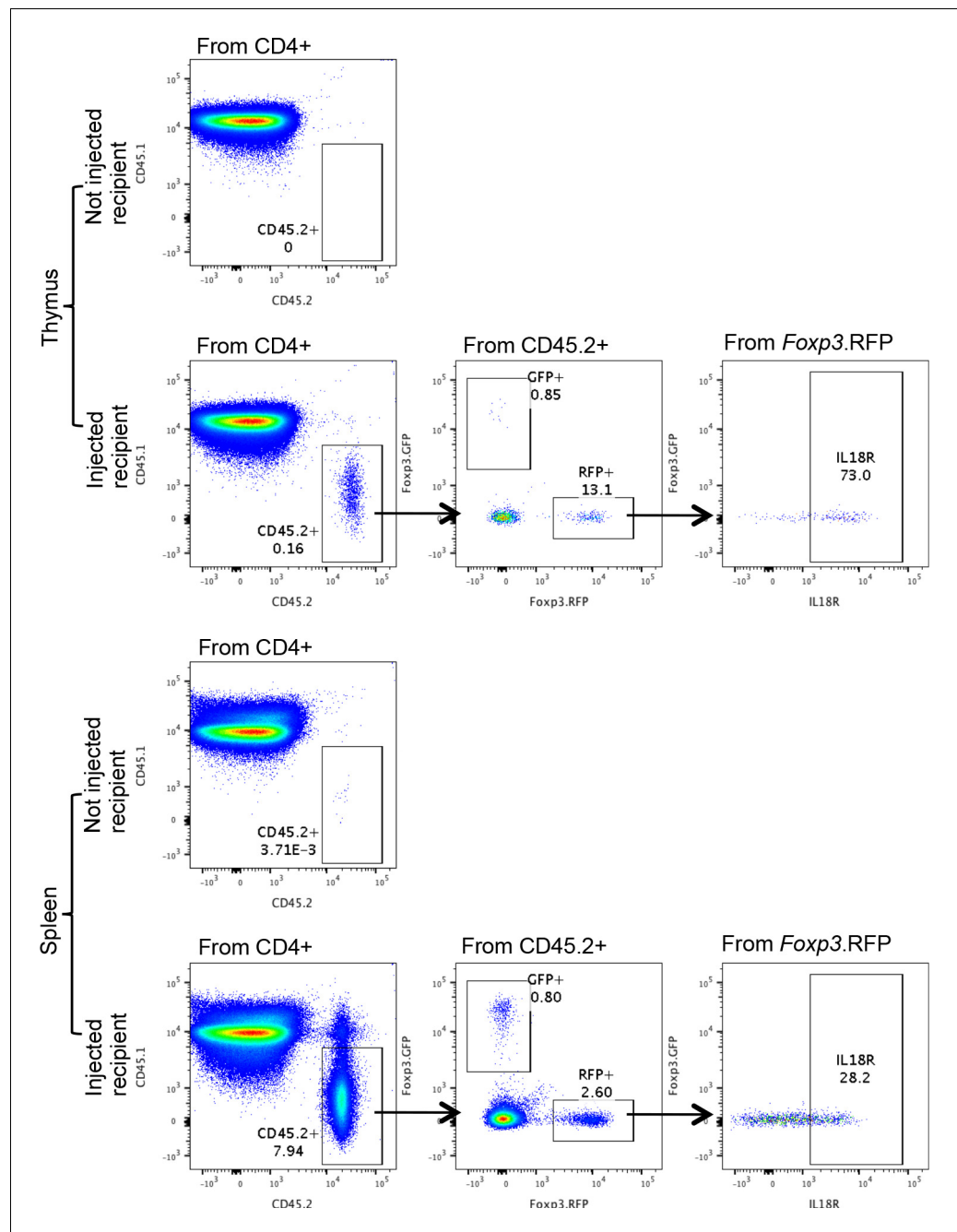


Figure 5—figure supplement 2. Representative gating from **Figure 5a,b,c**. Representative flow cytometry dot plots showing the gating of the injected CD45.2 cells (GFP and RFP) in the thymus (up) or the spleen (down) of CD45.1 recipients. Numbers indicate the percentage of cells within each gate.

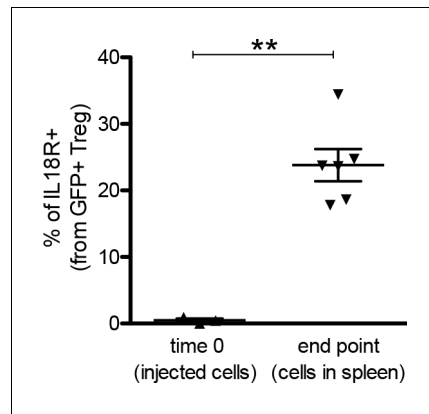


Figure 5—figure supplement 3. IL18R⁻ could give rise to IL18R⁺ Tregs. Frequency of IL18R in *Foxp3.GFP* Tregs at the time of injection to the recipient (time 0) and 12 days after the injection (end point). *Foxp3.GFP* Tregs were IL18R depleted before injection, and therefore frequencies of IL18R shown at time 0, also correspond to purity of the sorted cells. Each dot represents an individual mouse. The mean \pm SEM (standard error of the mean) is shown. Data are from three independent experiments with a total of 6 biological replicates. Significant differences were determined using a paired t-test and indicated by asterisks (** $p < 0.01$).

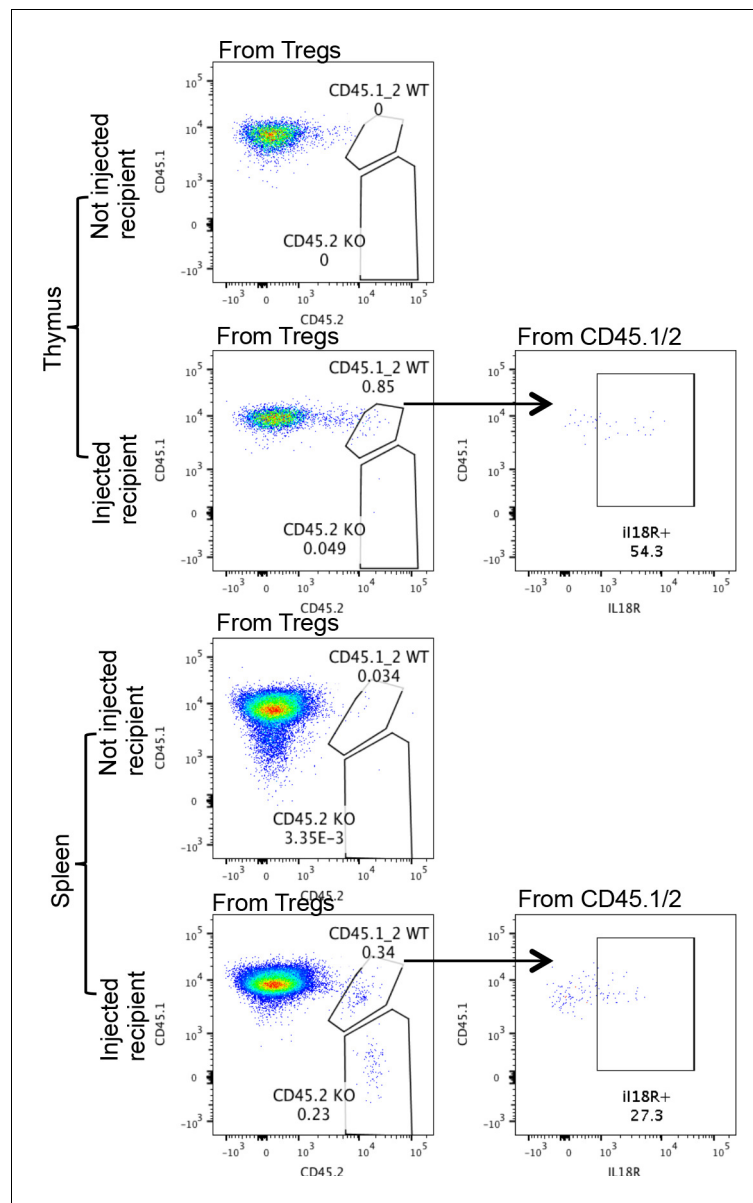


Figure 5—figure supplement 4. Representative gating from **Figure 5d,e,f**. Representative flow cytometry dot plots showing the gating of the injected CD45.2 cells (*Il18r1* KO) and CD45.1/2 cells (WT) in the thymus (up) or the spleen (down) of CD45.1 recipients. Numbers indicate the percentage of cells within each gate.

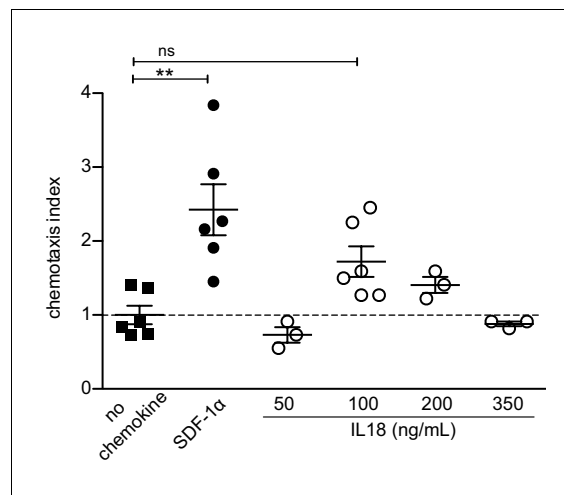


Figure 6. IL18 does not chemoattract Tregs. In vitro transwell chemotaxis assay showing migration of splenic Tregs in the presence of IL18 added to the lower wells at indicated doses. SDF-1 α (CXCL12) was added at a concentration of 100 ng/mL and served as a positive control. The mean \pm SEM (standard error of the mean) is shown. Data are from two independent experiments. The chemotaxis index was calculated as % migrated Tregs in the presence of stimulus/% migrated Tregs in the presence of medium alone (no chemokine). Significant differences were determined using ANOVA, corrected for multiple comparisons by the Bonferroni method and indicated by asterisks ** p <0.01, ns: non-significant.

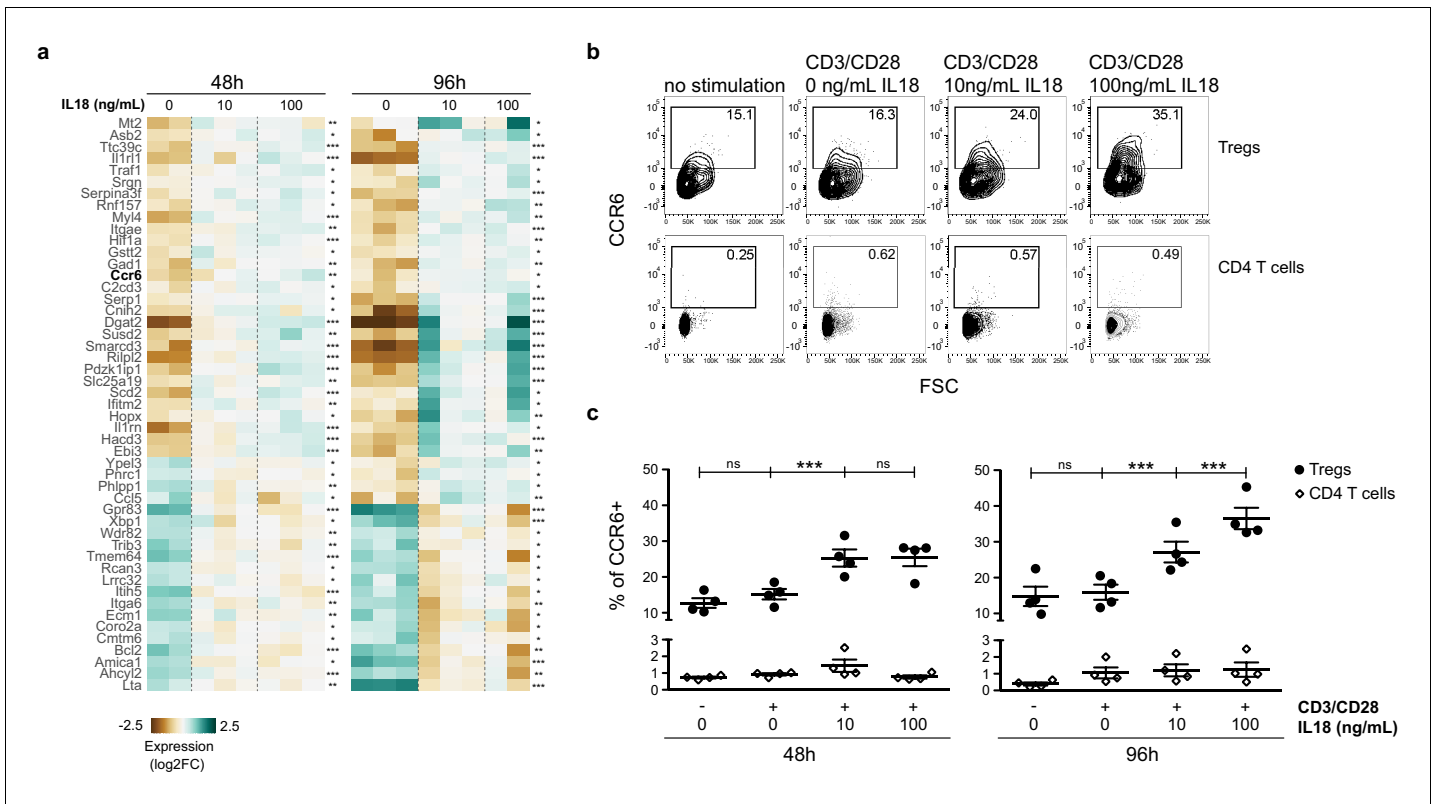


Figure 7. IL18/IL18R signaling upregulates CCR6. (a) A heatmap showing normalized expression of variable genes in splenic Tregs cultured with CD3/CD28 beads and absence/presence of IL18 (0, 10, 100 ng/mL). Selected genes have an adjusted p-value <0.1 in both 48 and 96 hr treatment versus control tests. Asterisks indicate adjusted p-values in each test *p<0.1, **p<0.01, ***p<0.001. (b) Representative flow cytometry plots showing CCR6 expression in CD25⁺FOXP3⁺Tregs (up) or CD25⁺FOXP3⁻CD4 T cells (down) cultured for 96 hr with no stimulation, CD3/CD28 beads, or CD3/CD28 beads plus absence/presence of IL18 (0, 10, 100 ng/mL). Numbers indicate the percentage of cells within each gate. (c) Frequency of CCR6 in CD25⁺FOXP3⁺Tregs (black dots) and CD25⁺FOXP3⁻CD4 T cells (empty rhombus) cultured for 48 or 96 hr with no stimulation, CD3/CD28 beads, or CD3/CD28 beads plus absence/presence of IL18 (0, 10, 100 ng/mL). Data are from two independent experiments with four biological replicates. Significant differences were determined using ANOVA, corrected for multiple comparisons using the Bonferroni method. For Tregs, differences are indicated by asterisks ***p<0.001, ns:non-significant. For CD4 T cells, ANOVA between conditions in both time-points was not significant.

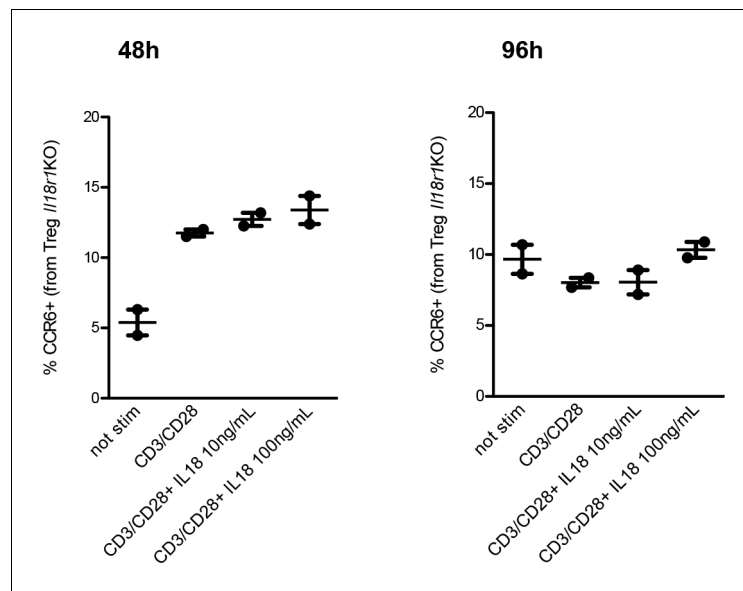


Figure 7—figure supplement 1. CCR6 upregulation upon IL18 is dependent on IL18R signaling. Frequency of CCR6 expression in Tregs from *Il18r1* KO mice cultured in vitro for 48 hr (left plot) or 96 hr (right plot) at different conditions (from left to right): not stimulated, stimulated with CD3/CD28 beads, stimulated with CD3/CD28 beads and IL18 10 ng/mL, and stimulated with CD3/CD28 beads and IL18 100 ng/mL. Data from two replicates are shown. The mean \pm SEM (standard error of the mean) is shown.